Materials Research Proceedings 41 (2024) 1850-1859 https://doi.org/10.21741/9781644903131-205

Axial drilling investigations and the potential of orbital techniques for enhanced hole quality in orthopedics

HUSSEIN Raafat[1,a*], ARAUJO Anna Carla[1,b], LANDON Yann[1,c] and RIBEIRO DA SILVA Cristiane Evelise[2,d]

[1]Institut Clément Ader (ICA), CNRS UMR 5312, Toulouse, France

[2]Materials Division, Instituto National de Tecnologia, Rio de Janeiro, Brazil

[a]raafat.hussein@univ-tlse3.fr, [b]araujo@insa-toulouse.fr, [c]yann.landon@univ-tlse3.fr, [d]cristiane.evelise@int.gov.br

Keywords: Biomanufacturing, Machining Bone, Drilling, Hole Accuracy, Delamination

Abstract. Precision in surgical bone drilling is essential for restoring bones mobility and function. However, the intricate nature and fiber-reinforced composite structure of bones inherently pose drilling-induced mechanical damage to the bone surface, affecting the primary stability necessary for implant anchorage and therefore leading to implant failure. The critical need for enhanced hole quality and damage reduction has spurred investigations into the optimal drilling parameters, novel drilling tools and alternative machining techniques. This study rigorously investigates the effect of the cutting speed and feed rate during axial drilling employing a center drill. It extends toward a comprehensive analysis of forces, temperature and mechanical damage, with a particular emphasis on delamination assessment. Then, the optimal parameters are established using the Tool-Material Couple (COM) optimization strategy. Subsequently, a novel approach of orbital drilling in bones is introduced for hole quality enhancement when compared to the conventional technique. This investigation serves as a foundational step for a more comprehensive study that ventures into the innovative application of orbital drilling in orthopedics.

Introduction

In orthopedic biomanufacturing, the optimization of drilling techniques holds paramount significance, particularly in the context of implant integration. Axial drilling has long been the conventional approach, necessitating a meticulous examination of tool specifications and drilling parameters to enhance hole accuracy and mitigate the adverse effects of delamination. The majority of drill bits and drilling techniques commonly employed in surgical procedures share design principles and geometric characteristics akin to those originally devised for metal cutting applications [1]. Consequently, addressing the inherent issues in conventional bone drilling remains challenging due to the intricate material properties of bones and the operational conditions involved. Therefore, for optimal hole quality, achieving a delicate balance among drilling techniques, parameters, and tool specifications is essential.

Over the past decade, researchers have extensively delved into the fundamental principles of bone cutting to enhance tool specifications and geometry. Liao et al. [2] introduced a milling cutter with a main cutting edge and micro-cutting edges arranged on an Archimedes spiral, combining fracture cutting with shear cutting and significantly reducing surface damage and cutting temperature. Shu et al. [3] proposed a three-step drill structure to modify cutting conditions at the entrance and exit of drilling aiming at reducing mechanical and thermal damages and improve position accuracy in bone drilling.

Drilling parameters play a critical role in bone drilling processes, affecting both temperature generation and drilling forces. Udiljak et al. [4] investigated high-speed drilling techniques to mitigate thermal damage, revealing that cutting speed had no discernible impact on axial drilling

force but significantly increased bone drilling temperature. Conversely, higher feed rate per tooth led to increased axial drilling force while reducing machining time and friction duration, resulting in lower temperatures. They recommended a minimum cutting speed of 6 m/min and a high drilling feed rate of 0.1 mm/tooth for effective temperature reduction in conventional drilling. Li et al. [5] further explored temperature trends, demonstrating that maximum temperature decreased with feed rate but increased with spindle speed. Simultaneously, exposure duration decreased with both feed rate and spindle speed. Samarasinghe et al. [6] observed contrasting effects of spindle speed and feed rate on temperature and force: higher spindle speeds increased temperature but minimized forces, whereas higher feed rates decreased temperature but maximized forces.

Singh et al. [7] conducted an analysis on the influence of different drilling methods, including conventional drilling (CD), ultrasonic-assisted drilling (UAD), and Robotic-assisted drilling (RAD) on bones. Their findings revealed significant reduction in thrust force when applying UAD compared to CD, as it increased hole dimension accuracy and reduced surface roughness. However, the ongoing quest for optimized hole quality and reduced heat generation in bone drilling techniques, has spurred researchers to explore alternative approaches [8]. In titanium alloys, CFRP, and aerospace materials, for example, orbital drilling has been widely used and demonstrated superior benefits over conventional and non-conventional drilling techniques due to its ability to reduce cutting forces and temperatures while improving hole quality [9]. However, to the author's knowledge, no studies have explored the application of orbital drilling in bones and its potential to enhance surgical procedures.

This paper presents a systematic investigation, substantiated by experimental data, to delineate the best conditions for axial drilling in orthopedics. The ultimate goal is to facilitate a future comparative analysis with orbital drilling and assess the potential need for procedural adjustments when employing robotic assistance in surgery. Axial drilling experiments were conducted on bone specimens using a center drill. The experimental procedure COM (Tool-Material Couple methodology) is used to define cutting speed and feed parameters. The results of hole quality of these experiments are analyzed to define the optimal range with higher precision. Additionally, some holes were drilled using orbital drilling technique to assess its efficiency compared to the conventional technique. This paper is an innovative work toward the unexplored domain of orbital drilling techniques in orthopedic applications.

Axial and Orbital Drilling Kinematics

Mechanistic force models offer a quantitative approach to predicting cutting forces based on the uncut chip thickness. Following experimental tests, these models facilitate the estimation of specific force coefficients for various sets of variables, as detailed in existing literature [10]. The forces in orthogonal cutting are delineated by a mechanistic force model that exclusively considers the cutting action of the cutting edge while neglecting ploughing and chisel edge effects. The machining force vector ($\vec{F}$) is computed by decomposing it into tangential (dF_t), radial (dF_r), and axial (dF_f) components for small elements of the cutting edge along the flute. The local force at a specific point on the cutting edge is a function of the uncut chip thickness (h) and the specific force coefficients (K_c, K_r, and K_f), given by Eq. 1.

$$dF_j = K_j . h . db \quad (1)$$

Here, j represents the tangential, radial and axial components (c, r and f) and the product $h.db$ represents the elementary uncut chip load calculated at the specific point over the elemental length (db) of the cutting edge. In drilling operations, the specific force coefficients are commonly identified in a global frame, generalized from the local reference in each tool rotation.

$$K_c = \frac{F_c}{A_c} = \frac{120 . P_c}{V_c . f_z . D} \quad (2)$$

$$K_f = \frac{F_f}{A_c} = \frac{F_f}{f_z.\frac{D}{2}} = \frac{F_z}{f_z.D} \quad (3)$$

The local specific force coefficients exhibit variability along the cutting edge due to changes in cutting speed and varying cutting angles. For a fixed tool geometry of two flutes (Z=2), an average specific force coefficient is calculated using the total chip load per cutting edge (A_c), where $A_c = \int h.db = f_z.D/2$, f_z is the axial feed per tooth or per cutting edge and D is the nominal tool diameter. Notably, experimental measurement of the cutting force for a single cutting edge is impractical in drilling, necessitating the consideration of both edges and their opposite directions. The average specific cutting force (K_c in N/mm²) for a tool-workpiece pair is then calculated using the experimental cutting power (P_c), incorporating contributions from both cutting edges as in Eq. 2. Conversely, measuring the total force in z direction (F_z) allows for the direct calculation of the feed force for each cutting edge (F_f), where $F_z = Z.F_f$, (Z=2). The specific feed force (K_f in N/mm²) is determined accordingly as in Eq. 3.

Orbital drilling, also called helical milling, introduces an innovative hole making technique in orthopedics where the end mill cutter traces a helical path around the hole axis within the workpiece. This method involves two primary movements: spindle rotation (N_{rev}) in round per minute (rpm) and the feed movement along the helical trajectory (Vf_{traj}) in mm per minute (mm/min), which can be decomposed into tangential feed (Vf_{xy}) and axial feed (Vf_z). The diameter of the helical path (D_e in (mm)) is determined by the hole diameter (D_H) and tool diameter (D_t) according to Eq. 4. Understanding cutting forces in orbital drilling necessitates defining four crucial parameters: the pitch (P in mm/rot), representing the axial depth per orbital rotation, the ramp angle (α) of the path, axial feed per tooth (f_z), and tangential feed per tooth (f_{xy}). The relationship between α, P, and e is described by Eq. 5, where P is a function of the feed as in Eq. 6. f_z and f_{xy} are local parameters used to determine the feed rate along the helical trajectory as in Eq. 7, where Z is the tooth number of the end mill.

$$D_e = 2e = D_H - D_t \quad (4)$$

$$\alpha = tan^{-1}\frac{P}{2.\pi.e} \quad (5)$$

$$P = \frac{f_z}{f_{xy}}.2.\pi.e \quad (6)$$

$$Vf_{traj} = N_{rev}.Z.\sqrt{{f_z}^2 + {f_{xy}}^2} \quad (7)$$

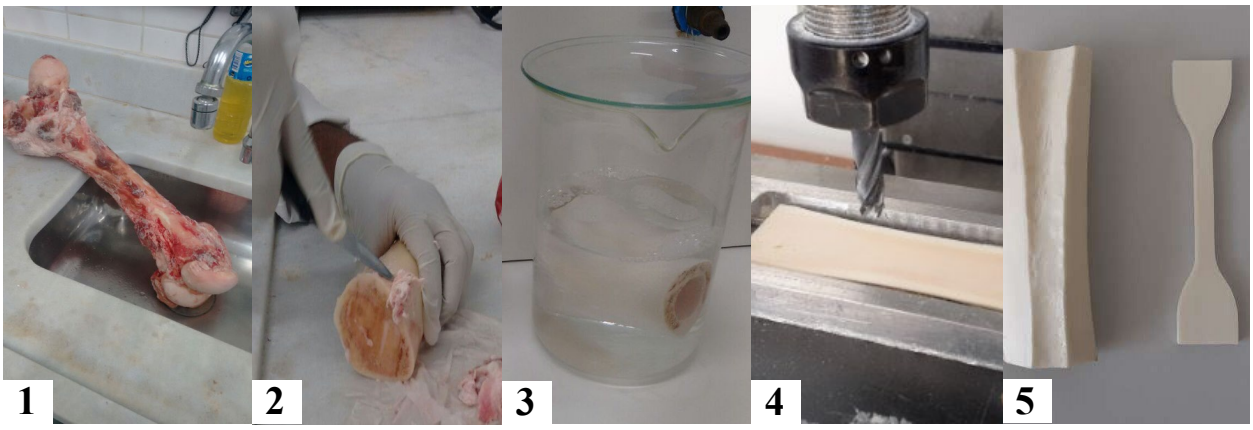

Figure 1: Bovine bone samples preparation.

Materials and Methods

The selection of bone specimens involved a meticulous process to ensure relevance to real-world clinical scenarios. This specific phase of the project was conducted in collaboration with the National Institute of Technology (INT) of Rio de Janeiro (Brazil), ensuring the highest standards of precision and adherence to scientific protocols throughout the sample preparation process. Bovine femurs (Fig. 1-1), which exhibit structural similarities to human bones, were obtained from a local slaughterhouse, specifically sourced from Nelore breed cattle aged 2 years. The bovine bones were derived ethically where no animals were harmed for the purpose of this in-vitro study.

The initial step of the preparatory procedure involved the precise removal of bone epiphyses, focusing exclusively on the bone diaphysis segment for subsequent sample preparation as shown is Fig. 1-2. Following this, a meticulous dissection procedure was implemented, encompassing comprehensive internal and external cleansing to eliminate bone marrow and soft tissue components. The thorough cleaning protocol employed a solution of hydrogen peroxide (35% p.a), as illustrated in Fig. 1-3, appropriately diluted with distilled water in a 50% ratio. This formulation was instrumental in achieving the efficient removal of soft tissue while preserving the integrity of the bone structure. After the cleansing process, each diaphysis femur underwent a precise division into four longitudinal sections, resulting in a total of 100 samples. Following the dissection and cleansing procedures, the prepared femur specimens underwent a milling procedure (Fig. 1-4) to refine their shape to have a tensile test geometry according to ASTM D638 standard, type IV (Fig. 1-5). Each sample, approximately measuring 25 mm (length) × 6.22 mm (width) with a thickness of 3.2 mm, emphasizing the need for meticulous control over the thickness (error = ±0.05 mm) to eliminate the thickness-induced error in the temperature elevation. This critical step aimed to ensure uniformity and compliance with standardized testing protocols for subsequent traction tests before drilling experiments to determine the bones specimens' elastic modulus. This step was crucial in characterizing the material mechanical properties of the bones, providing valuable data on their resistance to deformation under axial loading and their mechanical behavior.

Complementary to the traction tests, the density and specific heat of each bone specimen were measured. These parameters are essential for assessing thermal responses during the drilling process. The density data contributes to understanding the structural composition of the bone, while specific heat measurements provide insights into the material's thermal characteristics. The density was measured by Helium psychometry (Quantachrome Ultrapycnmeter 1000) with five measurements recorded for each sample. Heat capacity of the bovine bone sample, which represents the amount of heat required to raise the temperature of one gram of the bovine bone sample by one Kelvin, was determined through a simultaneous thermal analyzer, utilizing a sapphire standard for calibration. The properties listed in Table 1, including elastic modulus,

density, and specific heat, are crucial factors that vary among different types of bones and influence their drilling behavior. As bones exhibit a wide range of properties depending on factors such as bone density, mineral content, and microstructure, it is essential to account for these variations in the design and optimization of drilling processes for bone tissues [11]. The elastic modulus dictates bone stiffness and resistance to deformation during drilling, density influences material removal rates, chip formation, and tool wear and specific heat reflects the low thermal conductivity of bones which affects heat dissipation.

Table 1: Material characteristics of the bone samples.

Material properties	**Bovine bones specimens**
Elastic modulus	24 ± 1.15 [GPa]
Density	2.2799 ± 0.0151 [g/cc]
Specific heat	3.7796 ± 0.1038 [J/Kg°C]

The drilling experiments were executed on a CNC DMG-DMU85eVo, employing a rigorous methodology to ensure precision and accurate data acquisition. Workpieces were securely mounted onto a 9257B Kistler dynamometer, a 6-component force measurement device. This dynamometer, seamlessly connected to a 5070 Kistler amplifier, facilitated the meticulous capture and recording of forces generated during drilling experiments. For the acquisition of force data with utmost precision, a 9201 National Instruments acquisition module operating at a 10 kHz acquisition rate and employing analog-to-digital conversion was deployed. The entire data acquisition and analysis process were conducted using the LabView platform, ensuring a comprehensive understanding of drilling dynamics. All drilling tests were conducted at room temperature (approximately 25 °C). Type K thermocouples, with a temperature range of −40 °C to 500 °C, were inserted to measure temperature during the drilling operation. Thermocouple holes (diameter of 1.4 mm) were drilled on one side of the cross-section of specimens to position the thermocouple bead at a depth of 1.5 mm from the top bone surface and 1 mm from the surface of the hole wall (Fig. 2-a). Temperature data were recorded using the TC-08 data logger, connected to a USB port on the computer, and the Pico log software was utilized for data visualization. As the drilling depth did not extend to levels typically associated with significant thermal effects, especially considering the short duration of the longest experiment, which was less than 30 seconds, the study prioritized the comparison of the maximum temperature value achieved under each set of drilling conditions. Notably, manual irrigation methods, due to their limited efficiency in cooling during cortical bone drilling, and considering the small thickness of the specimens, were intentionally excluded from the current experimental setup.

A series of axial drilling experiments was executed using a 2-fluted, 4 mm-diameter solid carbide center drill from Fraisa (Fig. 2-b) to investigate the effect of such drill specifications on the mechanical damage. The conical shape and wider margin of center drills play a role in minimizing the risk of fractures or damage to the bone, ensuring a more controlled and accurate drilling procedure. The orbital drilling experiment was conducted as an insightful random test, allowing us to assess its efficiency and draw meaningful comparisons with axial drilling, despite the inherently distinct parameters associated with each technique. A 4-fluted, 3-mm-diameter end mill of 30º helix angle from Fraisa (Fig. 2-c) was used to conduct orbital drilling experiment at a cutting speed of 20 m/min, a local axial feed (f_z) of 0.008 mm/th and a local tangential feed (f_{xy}) of 0.09 mm/th.

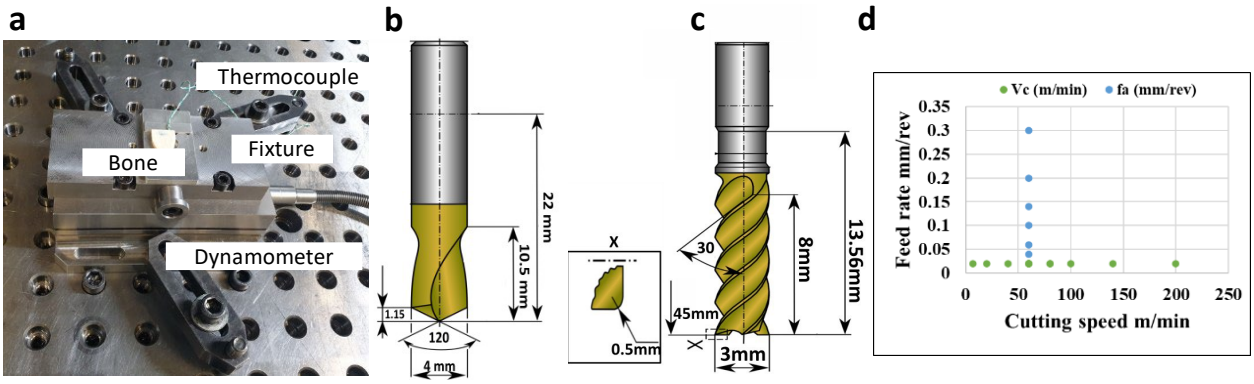

Figure 2: a) Experimental setup, b) center drill for axial drilling experiment, (c) end mill for orbital drilling experiment and d) design of experiment according to COM

The Tool-Material Couple (called as COM in French standard NF E66-520) is a methodical approach designed to establish the appropriate machining conditions for a given material. This standardized procedure consists in minimizing the specific cutting energy, and in the case of axial drilling, it relies on minimizing the specific axial coefficient, denoted as K_f. It is used in this case to analyze the quality requirements, such as, the delamination, where the operating conditions considered are the cutting speed (V_c in m/min) and axial feed (f_a in mm/rev). The maximum temperature achieved was also recorded in all experiments because the limiting temperature and heating time are important to avoid bone damage. Establishing the optimal tool operating domain involves a two-step process:

- First step involves adjusting the cutting speed while maintaining a fixed axial feed. The axial feed was maintained at a constant rate of 0.02 mm/rev and the cutting speed was changed in each experiment across a spectrum, including values of 6.5, 20, 40, 60, 80, 100, 140, and 200 m/min, each was repeated twice. The optimum cutting speed value is defined, during the experiment, to the one corresponding to the minimal delamination.
- Subsequently, the cutting speed was fixed at the optimum value determined in the previous step and the axial feed was increased for each experiment across a spectrum, including values of 0.04, 0.06, 0.1, 0.14, 0.2 and 0.3 mm/rev to determine the feed corresponding to the minimal delamination. Notably, each experiment was repeated twice.

During the drilling operations, forces and temperature were recorded and analyzed. Each drilled hole was then examined by a Dino-Lite Digital Microscope (AM8117MZT) to check the delamination around the hole edge. High-resolution images of the bone specimens, encompassing both pre- and post-drilling states on both sides, were acquired using an Olympus digital microscope. The analytical emphasis then shifted towards the precise identification and quantification of delamination areas through a combination of ImageJ and Python scripts, purposefully designed for image segmentation. The utilization of these scripts enabled thorough and detailed processing of the digital images, extracting crucial information for subsequent evaluation. The procedure for image segmentation can be described as follows (Fig. 3):

1. High-resolution microscope images of the specimen were captured before and after drilling.
2. Using Python, image segmentation was performed on both pre- and post-drilling images.
3. Both images were compared, and regions or pixels unrelated to the delaminated area were identified and removed.
4. The images were converted to grayscale to facilitate the marking of the delaminated area.
5. Image parameters, such as circle center and radius, were determined through methods like image enhancement and circle fitting. The least squares method was used to ensure the accurate fitting of the circle based on the detected edges.

6. Based on the determined circle parameters, the delamination was accurately extracted through threshold segmentation.
7. The images were then processed in ImageJ: the contrast was adjusted, the hole's area was removed, and further threshold segmentation was applied as shown in Fig. 3-2,3,4 respectively.
8. Noise filtering techniques were employed to refine the segmentation results Fig. 3-5.
9. As a result of these steps, only the delaminated area remained in the images.

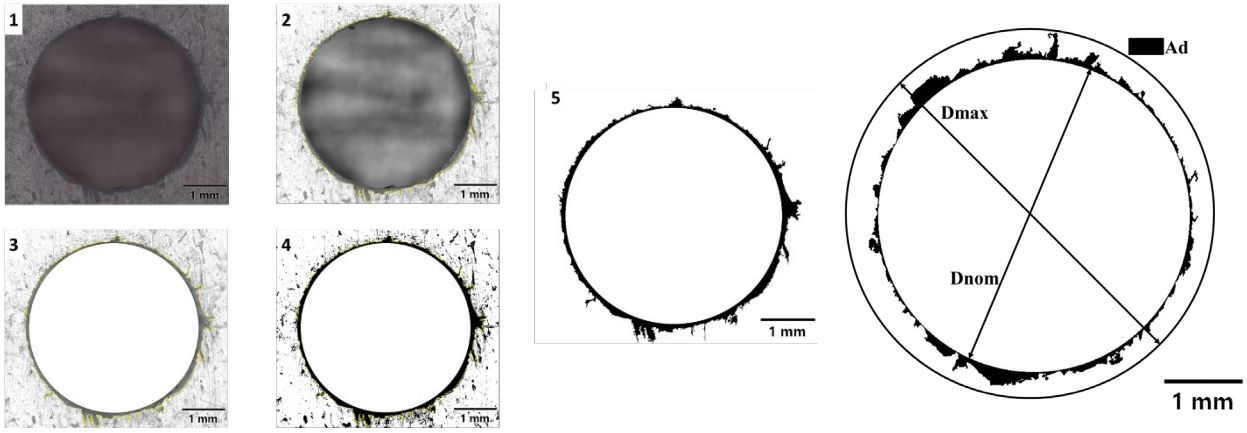

Figure 3: Image segmentation process to calculate the delaminated area around the hole.

Specific parameters crucial to the assessment of delamination were considered. The delamination factor (Fd) was proposed by [12] as the ratio of the maximum diameter of delamination (D_{max}) and the nominal diameter (D_0) as shown in Eq. 8. However, this conventional delamination factor fails to provide an accurate representation of delamination magnitude as it neglects the consideration of the area and severity of delamination. In response, [13] introduced an improved approach, termed the adjusted delamination factor (Fda), expressed in Eq. 9. Fda incorporates the conventional delamination factor (Fd) and a term reflecting the damaged area extent Ad as depicted in Fig. 3. Notably, it considers both the maximum crack length (A_{max}) and the initial area (A_0) corresponding to D_{max} and D_0, respectively.

$$Fd = \frac{D_{max}}{D_0} \tag{6}$$

$$Fda = Fd + \frac{Ad(Fd^2 - Fd)}{A_{max} - A_0} \tag{7}$$

Results and Discussion

Axial drilling experiments were conducted to assess the influence of cutting conditions, specifically cutting speed and axial feed, on the mechanical integrity of bone tissue, as denoted by hole quality. The examination of delamination, as depicted in Fig. 4, reveals a relationship between delamination and the cutting parameters. Both Fd and Fda exhibit an initial peak at lower cutting speeds, subsequently diminishing with the increase in cutting speed up to 60 m/min. However, an upswing is observed at 80 m/min, followed by a declining trend at higher cutting speeds, notably

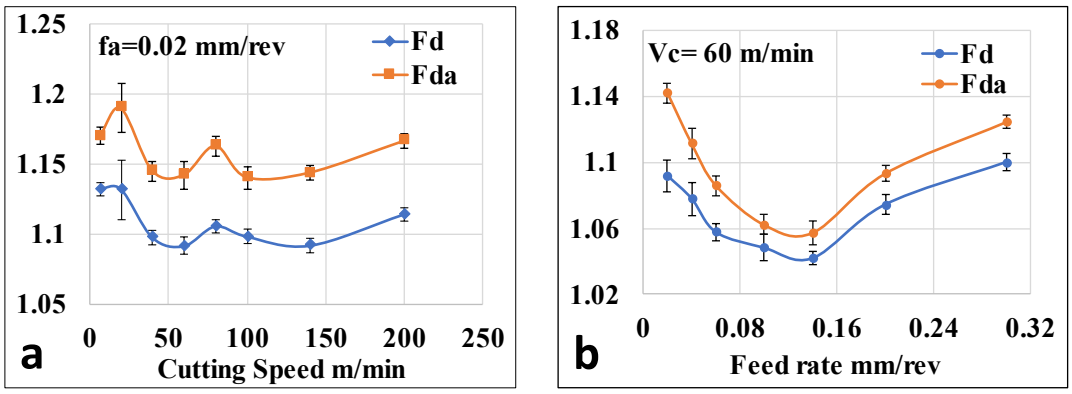

Figure 4. The effect of cutting speed and axial feed on

140 m/min. This evolution is difficult to explain. It can be assumed that at low cutting speeds, the cutting mechanism is degraded and ruled by ploughing effect, generating delamination more easily. At 80 m/min, the evolution of the delamination results indicates a change in the cutting mechanism, with probably higher forces and higher temperature generated in the drilling zone, leading to fiber and matrix softening. In contrast, delamination concerning the feed rate demonstrates a decreasing trend until reaching 0.14 mm/rev, after which a notable increase is observed. This can be explained by the axial force. At low feed rates, the ploughing effect due to the low chip thickness is preponderant and generates excessive axial forces. This phenomenon stabilizes around 0.08 mm/rev. Over 0.14 mm/rev, the increase of the feed leads to the increase of the axial force, as the mechanistic force models well represent it. Finally, the minimal delamination was observed at a cutting speed (V_c) of 60 m/min and an axial feed (f_a) of 0.14 mm/rev. Moreover, the observation from Fig. 4 reveals that the adjusted delamination Fda consistently surpasses the

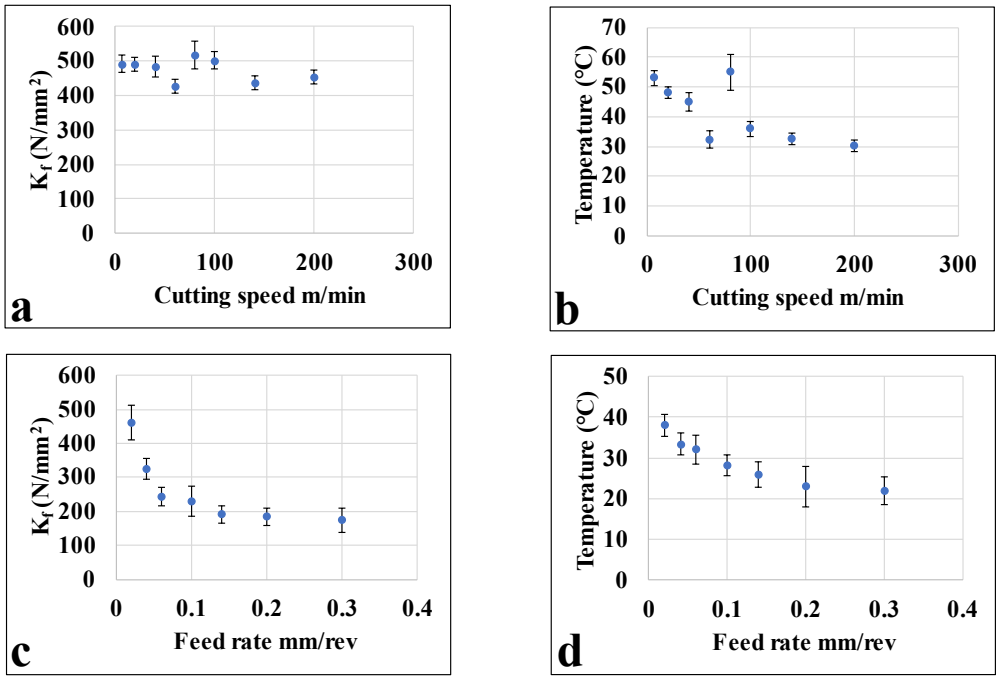

Figure 5. The effect of cutting conditions on the specific axial force coefficient and the maximum temperature.

conventional delamination factor Fd for all cutting speeds and feed rates. This superiority stems from the consideration of both the maximum crack length and the delaminated damaged area.

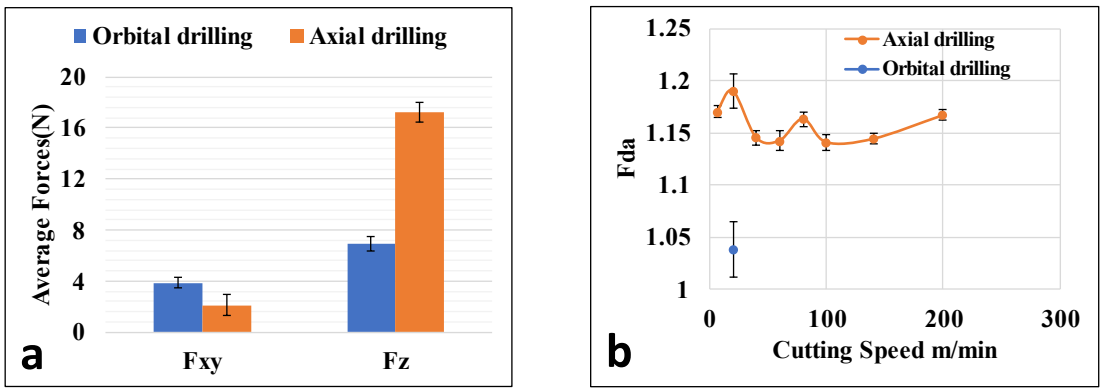

Figure 6. A Comparison between axial drlling technique under the optimized determined conditions of V_c=60 m/min and fa=0.14 mm/rev and orbital drilling technique under V_c=20 m/min, $f_z = 0.008$ and f_{xy} =0.09 mm/th according to the average forces and delamination.

The analysis of the specific axial force coefficient in axial drilling Fig. 5 reveals the lowest value reached at 60 m/min suggesting an optimal tool-bone interaction that balances tool penetration and chip formation. This confirms the previous analysis of the impact of the cutting speed on delamination. However, the non-uniform trend beyond 60 m/min may be attributed to the complex interaction of factors, including heat generation influencing bone properties and cutting dynamics. Conversely, the decreasing trend in the specific axial force coefficient with increasing feed rate indicates more efficient chip evacuation and reduced cutting resistance. The plateau observed at 0.14 mm/rev signifies an optimal feed rate where further increases have minimal impact. It can be related directly to the previous observations on delamination. This behavior also aligns with the parallel plateau response observed in maximal temperature, indicating a harmonized influence of feed rate on both cutting forces and heat generation.

The comparative analysis between orbital and axial drilling techniques is elucidated in Fig. 6. Orbital drilling reduces axial forces to approximately one-third of the corresponding axial forces in optimal axial drilling conditions. This reduction confirms the enhanced efficiency of orbital drilling and explains the results obtained for delamination indicating a reduction in the drilling-induced mechanical damage. The observed elevation in the tangential forces in orbital drilling is anticipated, given its inherent distribution of cutting forces between axial and tangential feeds. Moreover, the investigation into delamination reveals a noteworthy decrease of up to 9% when compared to delamination occurring at the optimal parameters of axial drilling. This reduction in delamination further emphasizes the advantages of orbital drilling, particularly in minimizing detrimental effects associated with mechanical damage during the drilling process, which in turn affects the primary implant stability. These findings show the potential of orbital drilling as an advanced technique with improved force characteristics and diminished delamination tendencies.

Conclusion

In this paper, the Tool-Material Couple (COM) optimization strategy was employed to establish the appropriate cutting speed and feed during axial drilling in cortical bones. This study aims to minimize mechanical damage and enhance the overall hole quality of bone. Results show that at a cutting speed (V_c) of 60 m/min and an axial feed (f_a) of 0.14 mm/rev a minimal delamination and cutting force coefficient with higher accuracy was detected. These findings provide insights into optimizing cutting conditions for minimal mechanical damage and efficient drilling performance in axial drilling applications for bones femur cortical bones as characterized in this study. Then, an orbital drilling experiment was conducted on bones to check the efficiency of this technique as an alternative to the conventional drilling techniques in orthopedics and it was clear that this novel

technique results in reduction of forces and elimination of delamination. Following the tendency of orbital drilling technique for mechanical damage reduction, an optimization strategy for the cutting parameters of orbital drilling is among the work perspectives of this study.

References

[1] Z. Jia, C. Zhang, F. Wang, R. Fu, and C. Chen, "An investigation of the effects of step drill geometry on drilling induced delamination and burr of Ti/CFRP stacks," *Composite Structures*, vol. 235, p. 111786, Mar. 2020. https://doi.org/10.1016/j.compstruct.2019.111786.

[2] Z. Liao, D. A. Axinte, and D. Gao, "A novel cutting tool design to avoid surface damage in bone machining," *International Journal of Machine Tools and Manufacture*, vol. 116, pp. 52–59, May 2017. https://doi.org/10.1016/j.ijmachtools.2017.01.003.

[3] L. Shu *et al.*, "A novel self-centring drill bit design for low-trauma bone drilling," *International Journal of Machine Tools and Manufacture*, vol. 154, p. 103568, Jul. 2020. https://doi.org/10.1016/j.ijmachtools.2020.103568.

[4] M. Can, S. Koluaçik, E. Bahçe, H. Gokce, and F. S. Tecellioglu, "Investigation of thermal damage in bone drilling: Hybrid processing method and pathological evaluation of existing methods," *Journal of the Mechanical Behavior of Biomedical Materials*, vol. 126, p. 105030, Feb. 2022. https://doi.org/10.1016/j.jmbbm.2021.105030.

[5] S. Li, L. Shu, T. Kizaki, W. Bai, M. Terashima, and N. Sugita, "Cortical bone drilling: A time series experimental analysis of thermal characteristics," *Journal of Manufacturing Processes*, vol. 64, pp. 606–619, Apr. 2021. https://doi.org/10.1016/j.jmapro.2021.01.046.

[6] H. Tian, X. Dang, D. Meng, B. Tian, and J. Li, "Influence of drilling parameters on bone drilling force and temperature by FE simulation and parameters optimization based Taguchi method," *Alexandria Engineering Journal*, vol. 75, pp. 115–126, Jul. 2023. https://doi.org/10.1016/j.aej.2023.05.048.

[7] G. Singh, A. Babbar, V. Jain, and D. Gupta, "Comparative statement for diametric delamination in drilling of cortical bone with conventional and ultrasonic assisted drilling techniques," *Journal of Orthopaedics*, vol. 25, pp. 53–58, May 2021. https://doi.org/10.1016/j.jor.2021.03.017.

[8] M. F. A. Akhbar and A. R. Yusoff, "Drilling of bone: thermal osteonecrosis regions induced by drilling parameters," *Biomed. Phys. Eng. Express*, vol. 5, no. 6, p. 065003, Sep. 2019.

[9] S. Akula, S. N. Nayak, G. Bolar, and V. Managuli, "Comparison of conventional drilling and helical milling for hole making in Ti6Al4V titanium alloy under sustainable dry condition," *Manufacturing Rev.*, vol. 8, p. 12, 2021. https://doi.org/10.1051/mfreview/2021010.

[10] J. C. Roukema and Y. Altintas, "Generalized modeling of drilling vibrations. Part I: Time domain model of drilling kinematics, dynamics and hole formation," *International Journal of Machine Tools and Manufacture*, vol. 47, no. 9, pp. 1455–1473, Jul. 2007.

[11]R. Hussein, Y. Landon, and A. C. Araujo, *BONE PROPERTIES - A REVIEW FOR DRILLING APPLICATION*. 2023. doi: 10.26678/ABCM.COBEF2023.COF23-0563.

[12] W.-C. Chen, "Some experimental investigations in the drilling of carbon fiber-reinforced plastic (CFRP) composite laminates," *International Journal of Machine Tools and Manufacture*, vol. 37, no. 8, pp. 1097–1108, Aug. 1997.

[13] J. P. Davim, J. Campos Rubio, and A. Abrao, "A novel approach based on digital image analysis to evaluate the delamination factor after drilling composite laminates," *Composites Science and Technology - COMPOSITES SCI TECHNOL*, vol. 67, pp. 1939–1945, Jul. 2007.